

Hydration characteristics of waste sludge ash that is reused in eco-cement clinkers

K.L. Lin^{a,*}, K.Y. Chiang^b, C.Y. Lin^c

^aDepartment of Environmental Engineering, National I-Lan University, I-Lan 260, Taiwan, ROC

^bDepartment of Environmental Engineering and Science, Feng-Chia University, Tai-chung407, Taiwan, ROC

^cWaste Minimization Division, Foundation of Taiwan Industry Service, Taipei 198, Taiwan, ROC

Received 22 January 2004; accepted 23 November 2004

Abstract

The study reports on the hydration characteristics of eco-cement clinkers produced with waste sludge ash as raw components. The tested mixtures were composed of different types of waste sludge ash, including sewage sludge ash, water purification sludge ash, limestone, and ferrate, prepared using the optimum proportioning method. The mixtures were burned at 1400 °C for 6 h. The clinkers thus obtained were quantified and the hydration characteristics of the eco-cement pastes prepared from the waste sludge ashes. The setting time, compressive strength, hydrates and porosity distribution were examined at various ages. The 28-day compressive strength of the early high strength developing of eco-cement C paste outperformed that of ordinary Portland cement paste by 3 MPa. It is supposed that the large quantity of limestone used provided CaO, which in turn enhanced the formation of C₃S, leading to the greater compressive strength development in the eco-cement C paste. From the porosity distribution, shown by the Mercury Intrusion Porosimetry results, it was found that, with increasing curing ages, the gel pores (<0.01 μm) increased and the total porosity and capillary pores (>0.01 μm) decreased—a result that shows that hydrates had filled the pores. This resulting densification and enhanced later strength were caused by the shifting of the pore size distribution to a smaller diameter range.

© 2005 Elsevier Ltd. All rights reserved.

Keywords: Compressive strength; Eco-cement; Hydration; Mercury porosimetry; Pore size distribution

1. Introduction

Increasing demands on natural resources and a scarcity of environmentally acceptable solid waste disposal sites are hastening many municipalities in Taiwan to consider resource recovery as an alternative. The annual sludge production from Taiwan in 29 purification treatment plants and 22 sewage treatment plants is 160,000 tons and 180,000 tons, respectively. Currently sanitary landfills are commonly used for the disposal of this sludge but rapid

urbanization has made it increasingly difficult to find suitable landfill sites [1].

Currently, the most common methods of sludge disposal are in ocean or land fills, or for agricultural purposes. In recent years, studies had been carried out by various researchers investigating the use of sludge as construction material. Tay [2,3] found that sludge mixed with clay could be used in the production of bricks for construction use. The sewage sludge ash (SSA) retained in filters can be deposited in controlled landfills or used in construction to improve some of the properties of the building materials. Incineration residues, such as rice husk ash [4,5] and municipal solid waste ash [6], have been used successfully in construction. SSA has been used in mortars [7], in concrete mixtures [8,9], in brick manufacture [10], as a fine aggregate in mortars [11], and

* Corresponding author. Tel.: +886 3 9357400x749; fax: +886 3 9367642.

E-mail address: kllin@niu.edu.tw (K.L. Lin).

Table 1
Chemical analysis of the raw materials

Composition	Primarily sewage sludge ash	Water purification sludge ash	Limestone	Ferrate
SiO ₂ (%)	63.31	54.47	3.76	6.61
Al ₂ O ₃ (%)	15.38	29.12	1.10	2.25
Fe ₂ O ₃ (%)	6.81	7.25	0.66	62.30
CaO (%)	1.80	0.93	52.46	0.71
MgO (%)	1.03	1.12	1.23	0.23
SO ₃ (%)	1.01	0.08	0.18	0.82
Na ₂ O (%)	0.70	0.67	0.22	ND
K ₂ O (%)	1.51	3.55	0.01	ND
P ₂ O ₅ (%)	7.20	ND ^a	ND	ND
Cl ⁻ (ppm)	105	311	ND	ND
Cu (mg/Kg)	5420	150	ND	ND
Cr (mg/Kg)	20	ND	ND	ND
Cd (mg/Kg)	20	ND	ND	ND
Pb (mg/Kg)	740	50	210	730
Ni (mg/Kg)	310	ND	ND	850
Zn (mg/Kg)	3510	110	1150	1320

^a ND: not detected.

in asphalt paving mixes [12]. The reuse of a waste in cement production mainly depends on the chemical composition of the waste. The major components in sewage sludge ash and water purification sludge ash, SiO₂, CaO, Al₂O₃ and Fe₂O₃ [13,14] can through the burning process, produce such compounds as calcium aluminates and calcium silicates, which include C₃S, C₂S and C₃A. Such compounds, which also commonly present in ordinary Portland cement, may function as binders or possess hardening characteristics.

A new type of Portland cement has been developed not only to solve the landfill sites problem, but also to conserve the environment by the resources circulation. This new type of cement is called “eco-cement”. It is the compound word of “Ecology” and “Cement” [15]. It has been expected greatly for the conservation of energy and environment by virtue of decreasing energy necessary for production, reducing CO₂ emission, reducing the natural resources for cement and reducing the load to disposal sites. In view of the aforementioned disposal problems and the increasing cost of construction materials, laboratory studies have been conducted to evaluate the use potential of sludge clinkers as a cement replacement material. The study discussed in this paper reports on the hydration characteristics of waste sludge that is reused in eco-cement clinkers. The tested mixtures were composed of different types of waste sludge, including sewage sludge ash, water purification sludge ash, limestone and ferrate, which were prepared using the optimum proportioning method. The mixtures were burned at 1400 °C for 6 h. The clinkers thus obtained were quantified and the hydration characteristics of the eco-cement pastes prepared from the waste sludge examined at various ages, including the compressive strength, hydrates and porosity distribution.

2. Materials and methods

2.1. Clinker preparation

A pilot-scale test was conducted to study the possibility of applying this technology in actual practice.

Water purification sludge ash and sewage sludge ash, limestone, and ferrate were used as raw materials in the tests. The oxide compositions of these raw materials, on a loss free basis, are given in Table 1. A computational model [14] was used to formulate the composition of the raw clinkers.

The raw materials were blended using three different ratios: eco-cement A, eco-cement B, and eco-cement C. Each cement clinker ratio was determined after considering the hydration modulus, $[HM=(CaO/SiO_2+Al_2O_3+Fe_2O_3), 1.7<HM<2.3]$, the lime saturation factor $[LSF=(CaO/SiO_2+1.18Al_2O_3+0.65Fe_2O_3), 0.8<LSF<0.95]$, the silica modulus $[SM=(SiO_2/Al_2O_3+Fe_2O_3), 1.9<SM<3.2]$, and the iron modulus $[IM=(Al_2O_3/Fe_2O_3), 1.7<IM<2.5]$. The four unknowns could be solved by 1st order simultaneous equations. The blend ratios are shown in Table 2.

The burning process is summarized as follows: incinerated ash of sewage sludge and water purification sludge ash was separated, dried and pulverized in a pretreatment process. The pretreated incinerated ash was mixed with other raw materials (e.g. ferrate) and supplements (e.g. limestone). The ground mixtures were burned in a programmable electrical furnace. The compound material was burned for 6 h at 1400 °C to form eco-cement clinker. After the burning process, the resultant clinkers were cooled in a clinker cooler, then mixed with plaster (e.g. 3.5% gypsum) and pulverized to produce eco-cement clinker. The fraction passing through a #325 mesh was then analyzed to determine its principal properties (shown in Table 1).

The cement used in this research was ordinary Portland cement (OPC) Type I, supplied by the Taiwan Cement Company. The major composition of the OPC is listed in Table 3.

Table 2
Blend ratios (wt.%) of the raw materials

Type of blend	Eco-cement A	Eco-cement B	Eco-cement C
<i>Type of blend</i>			
Sewage sludge ash	4.69%	8.98%	4.24%
Water purification sludge ash	13.03%	9.34%	12.45%
Ferrate	1.88%	2.08%	1.85%
Limestone	80.40%	79.60%	81.45%
<i>Modulus</i>			
LSF	0.92	0.84	0.95
HM	2.03	1.9	2.11
SM	1.99	2.3	2.1
IM	2.00	1.74	1.97

Table 3
Chemical composition of the OPC and eco-cement clinkers

	OPC	Eco-cement A	Eco-cement B	Eco-cement C
<i>Composition</i>				
SiO ₂ (%)	20.04	21.24	23.15	20.93
Al ₂ O ₃ (%)	5.35	7.11	6.39	6.60
Fe ₂ O ₃ (%)	3.44	3.55	3.67	3.35
CaO (%)	63.16	64.83	63.12	65.23
MgO (%)	2.31	1.28	1.11	1.17
SO ₃ (%)	2.03	3.24	3.27	3.51
R ₂ O (%) ^a	0.56	0.72	0.26	0.56
TiO ₂ (%)	0.27	0.33	0.31	0.27
P ₂ O ₅ (%)	ND ^b	0.46	0.75	0.21
Free CaO (%)	0.23	0.30	0.20	0.40
Ignition loss (%)	0.85	0.94	0.96	0.93
<i>Constituents</i>				
C ₃ S	51.01	48.65	31.74	56.91
C ₂ S	23.21	24.20	42.47	17.07
C ₃ A	8.21	12.83	10.72	11.82
C ₄ AF	10.32	10.80	11.17	10.19

^a R₂O: Na₂O+0.659 K₂O.

^b ND: not detected.

2.2. Approach

Three types of eco-cement clinkers prepared as above were used. Pastes using the aforementioned blends were prepared with a water to binder ratio of 0.38. 25.4×25.4×25.4 mm (1×1×1 in.) test cubes were prepared according to ASTM-305, followed by a mould-

Table 4
Heavy metal concentrations in TCLP leachates for the OPC and the eco-cement clinkers

	Cu (mg/L)	Cr (mg/L)	Cd (mg/L)	Pb (mg/L)	Ni (mg/L)	Zn (mg/L)
OPC	ND ^a	ND ^b	ND ^c	0.7	ND ^d	0.3
Eco-cement A	ND	ND	ND	0.6	ND	0.3
Eco-cement B	ND	ND	ND	0.6	ND	0.3
Eco-cement C	ND	ND	ND	0.6	ND	0.3
Regulatory thresholds	–	1.0	1.0	5.0	–	–

^a Detection limits<0.020 mg/L.

^b Detection limits<0.016 mg/L.

^c Detection limits<0.014 mg/L.

^d Detection limits<0.014 mg/L.

ing process (ASTM C31-69). The specimens were then demoulded and cured in a container at 95% humidity at 25 °C for 3–28 days. The compressive strength development of three samples was measured for specimens of each types of eco-cement pastes at different ages, according to ASTM C39-72. The leachability of the specimens was analyzed by Toxicity Characteristic Leaching Procedure (TCLP) tests. The chemical composition was analyzed, using X-ray fluorescence (XRF) techniques. The composition changes and hydration characteristics were analyzed, using both the XRD and MIP techniques, for pulverized and sieved (#300) samples whose hydration was terminated at the tested age with acetone under a vacuum for 24 h.

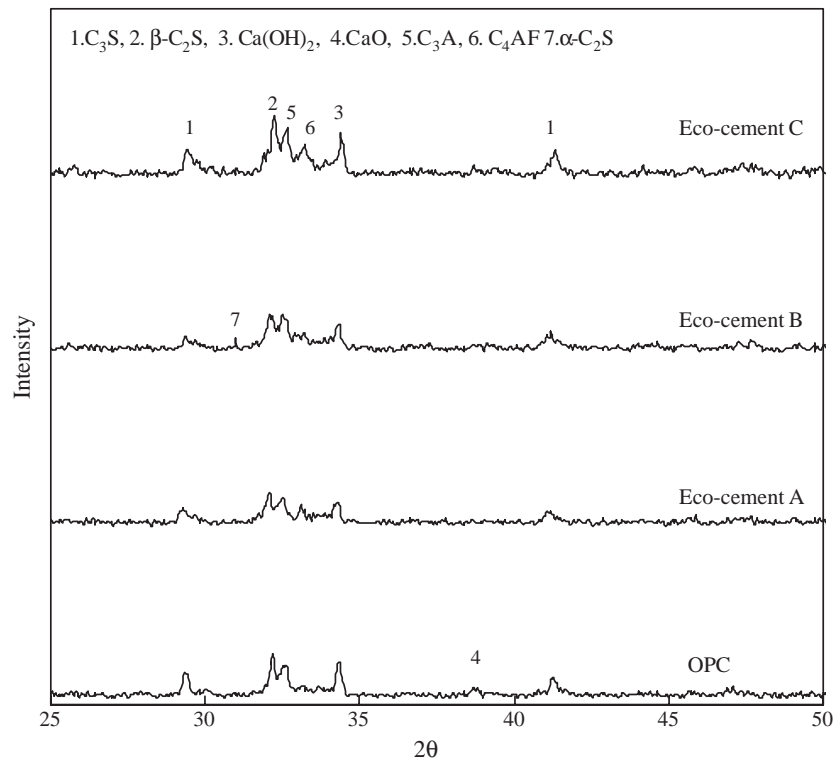


Fig. 1. XRD patterns of the OPC and eco-cement clinkers.

Table 5
Setting times for OPC and eco-cement pastes

Paste	Initial setting (h)	Final setting (h)
OPC	3.20	5.28
Eco-cement A	4.27	5.92
Eco-cement B	8.80	10.85
Eco-cement C	1.68	3.13

2.3. Analyses

Chemical and physical analyses of the ordinary Portland cement and the three types of eco-cement pastes were conducted at different ages as follows:

- Unconfined compressive strength (UCS): ASTM C39-72.
- Heavy metal leachability (TCLP): SW-864-1311.
- Heavy metal concentration: Cd (SW864-7131A), Pb (SW864-7421), Zn (SW864-7951), Cu (SW864-7211), Cr (SW864-7191).
- Setting time: the setting times of the cement mixes were determined according to ASTM C191 using a Vicat apparatus at room temperature. The initial setting time was defined as when a Vicat needle 1 mm in diameter would penetrate the sample to a point 5 ± 1 mm from the bottom of the mould. The final setting time was defined as when a 5-mm cap ring would leave no visible mark when placed on the surface of the sample.
- Mineralogy: the XRD analysis were carried out by a Siemens D-5000X-ray diffractometer with $\text{CuK}\alpha$ radiation and 2θ scanning, ranging between 10° and 50° .
- Chemical composition: the X-ray fluorescence (XRF) was performed with an automated RIX 2000 spectrometer. The specimens were prepared for XRF analysis by mixing 0.4 g of the sample and 4 g of 100 Spectroflux, at

a dilution ratio of 1:10. Homogenized mixtures, were placed in Pt–Au crucibles, then treated for 1 h at 1000°C in an electric furnace. The homogeneous melted sample was recast into glass beads 2 mm thick, and 32 mm in diameter [16].

3. Results and discussion

3.1. Characterization of the eco-cement clinkers

The X-ray diffraction patterns of the OPC and the eco-cement clinkers are illustrated in Fig. 1, showing the speciation. The major components of the Portland cement, C_3S (i.e., $3\text{CaO}\cdot\text{SiO}_2$), C_2S (i.e., $2\text{CaO}\cdot\text{SiO}_2$), C_3A (i.e., $3\text{CaO}\cdot\text{Al}_2\text{O}_3$), and C_4AF (i.e., $4\text{CaO}\cdot\text{Al}_2\text{O}_3\cdot\text{Fe}_2\text{O}_3$), were all found in both the eco-cement A clinker and eco-cement C clinker. Eco-cement B clinker also showed the formation of $\alpha\text{-C}_2\text{S}$ phase.

The properties of the three types of eco-cement clinker used in this study were analyzed. The XRF analysis results are summarized in Table 3. It is noted that SiO_2 , CaO , Al_2O_3 were the primary components found in the eco-cement clinkers. The belite content in the eco-cement A clinker was similar that in the OPC. Phase compositions were predicted theoretically using a modified Bogue calculation. These are given in Table 3.

Table 3 indicates that the clinker produced from eco-cement B contained larger amount of belite and a smaller amount of alite. It is believed that the phosphate in the raw material did not decompose during the burning process and was fixed in the final product. Normally the P_2O_5 content in Portland cement is as much as 0.2%, but cements produced from clinker had 0.5% P_2O_5 , leading to lower

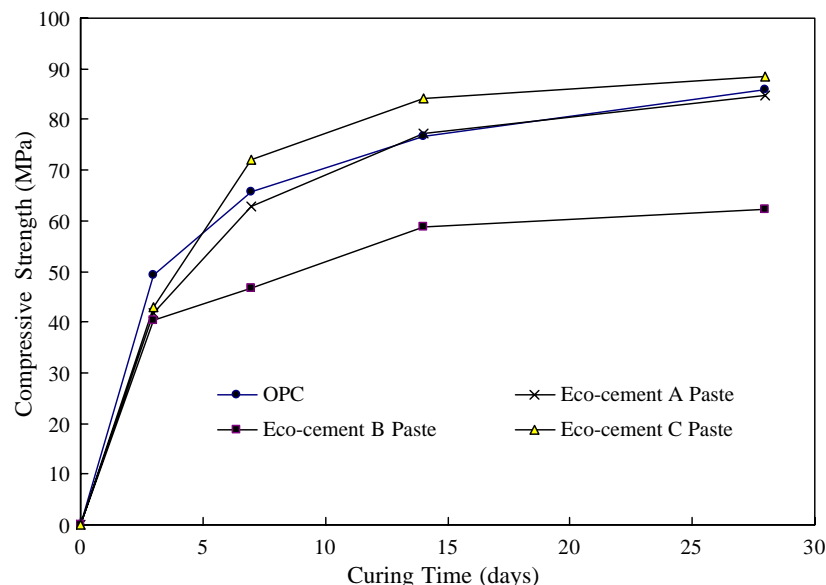


Fig. 2. Compressive strength development of the OPC and eco-cement pastes.

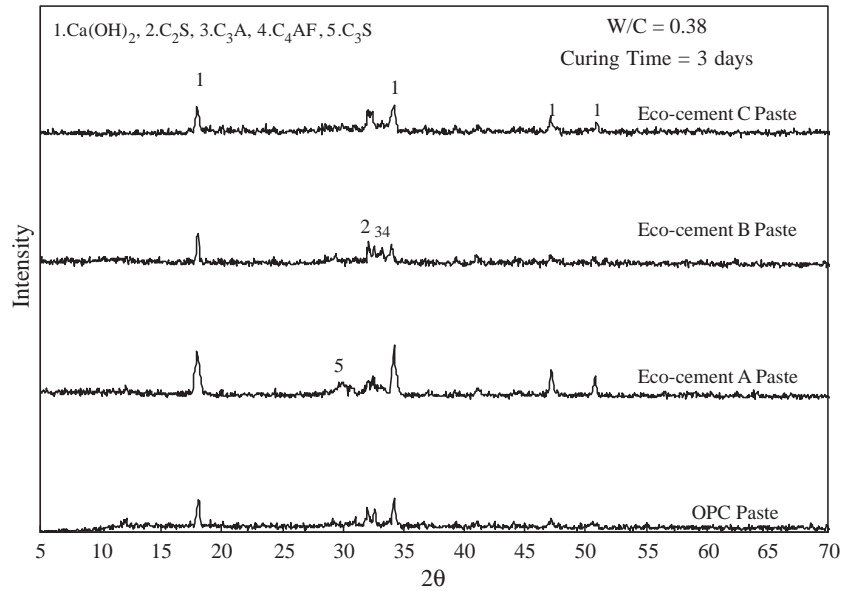


Fig. 3. XRD patterns of the OPC and eco-cement pastes at 3 days.

strength due to the decomposition of C_3S , obtaining $\alpha\text{-C}_2\text{S}$ rich in P_2O_5 [17]. Increasing the P_2O_5 content increases the free-CaO content and lowers the $\text{C}_3\text{S}/\text{C}_2\text{S}$ rate [18]. The clinker produced from eco-cement C had greater amount of alite. The oxides Na_2O and K_2O , so called alkalis, are normal components of all the eco-cement clinkers [18]. The alkalis content in Portland cement is usually 0.5–1.3%.

All the tested eco-cement clinkers met the TCLP requirements. There was a high heavy metal content, which included Pb, Zn, Cd, Ni, Cr and Cu (See Table 1). But it was found that the leaching concentrations all met the regulatory thresholds (see Table 4).

3.2. Setting times of the OPC and eco-cement pastes

As the cementitious hydraulic reactions progress, cement hardens and develops its strength. Basically, the setting behavior is a result of the cement grains dispersing (dissolving) and hydrating in the water, to gradually form a solid/liquid suspension of the various hydrates. As the process continues, the inner structure of the cement paste is further reinforced to become a network structure, which causes the cement to set and gain strength.

The setting times for the three types of OPC and the eco-cement pastes are given in Table 5. The results show that eco-cement A paste had a bigger initial setting time and final

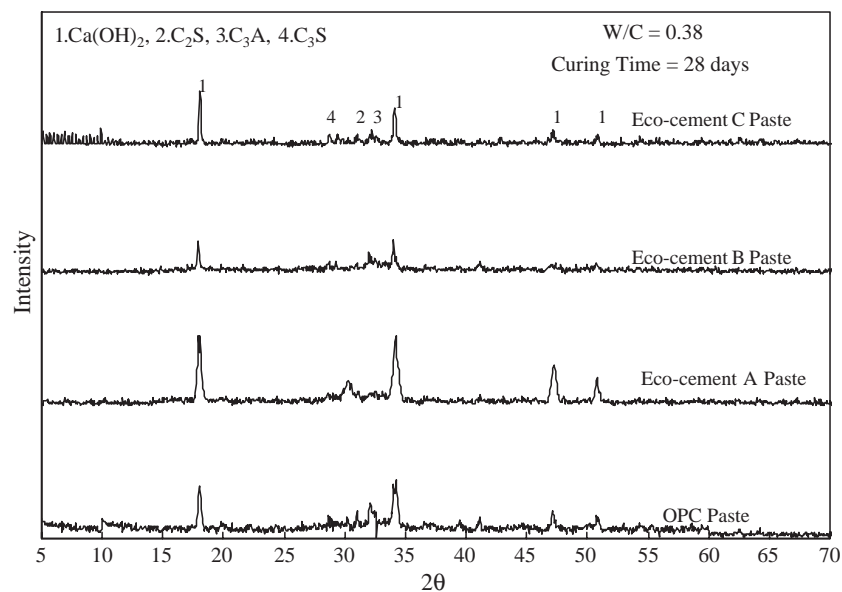


Fig. 4. XRD patterns of the OPC and eco-cement pastes at 28 days.

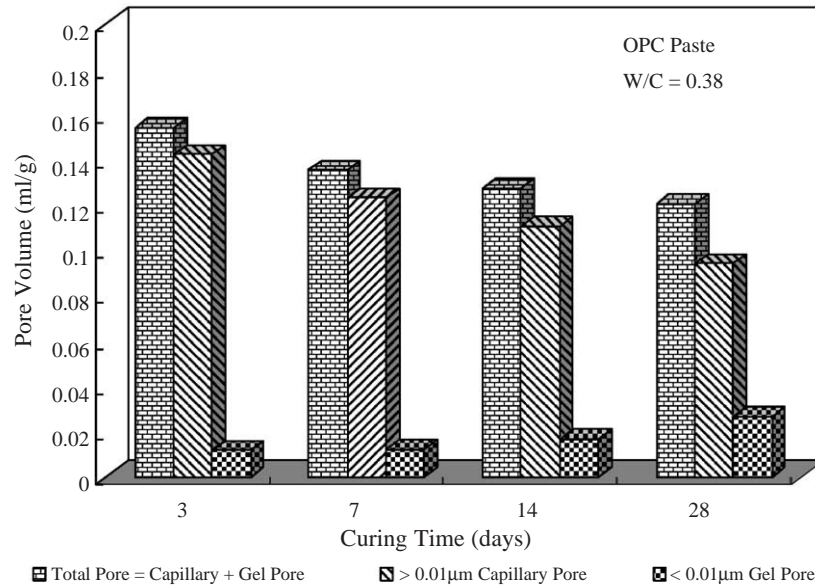


Fig. 5. Pore size distribution in OPC pastes.

setting time to OPC paste. Eco-cement B paste had a delayed setting time, which may be attributed primarily to the large amount of α -C₂S. The accelerated setting of eco-cement C paste could be attributed to more C₃S. The setting time of the eco-cement C paste was shorter, thereby decreasing its workability.

3.3. Compressive strength development of the OPC and eco-cement pastes

Fig. 2 shows the compressive strength of the OPC and eco-cement pastes. It can be observed that the compressive strengths of OPC and all three types of eco-cement pastes occurred within the curing times (3 to 28 days). At 28 days, the strength of eco-cement A paste was similar to that of

OPC paste. The experimental results indicate that eco-cement B paste had a slower compressive strength development. It can be noticed that the eco-cement B clinker contained larger amounts of α -C₂S, which led to lower compressive strengths, relative to the OPC paste. The experimental results indicate that eco-cement C paste showed a slower compressive strength development at 3 days, but at 28 days, the strength was 3 MPa, which exceeds that of OPC paste.

3.4. OPC and eco-cement paste hydrates

Figs. 3 and 4 show the XRD analyses of the hydrates of OPC and three types of eco-cement pastes, at 3 days and 28 days, respectively. We can see that the main hydration

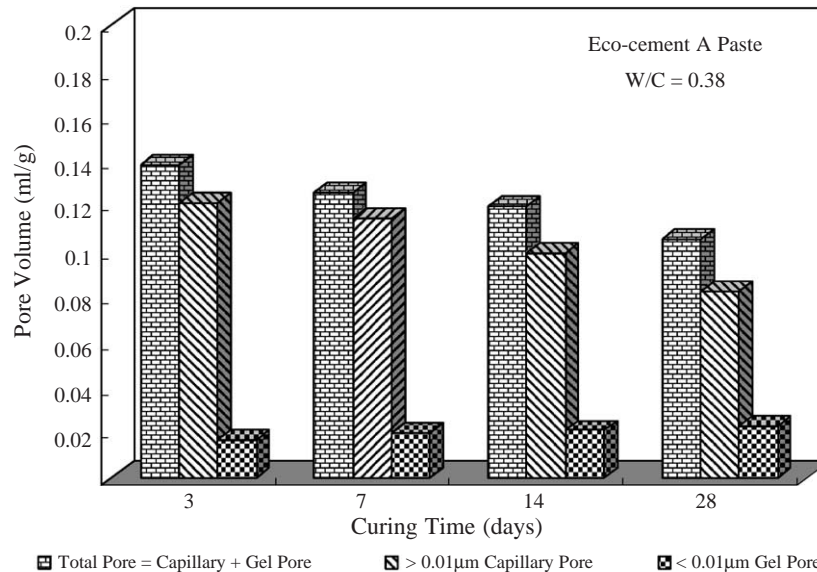


Fig. 6. Pore size distribution in eco-cement A pastes.

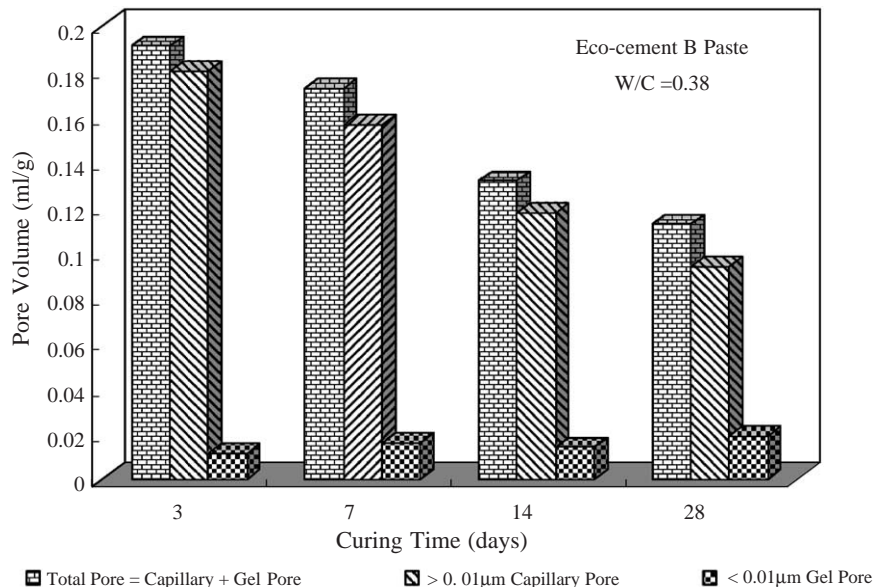


Fig. 7. Pore size distribution in eco-cement B pastes.

products in the pure cement were C–S–H gels, $\text{Ca}(\text{OH})_2$, and unhydrated C_3S and C_2S (See Fig. 3). In eco-cement A paste, the hydration products in the mixture were the same as those in pure cement. Fig. 4 shows the XRD patterns of eco-cement pastes hydrated for 28 days. By comparing Fig. 3 with Fig. 4, we find that the intensities peaks of the eco-cement A pastes and eco-cement C pastes of the $\text{Ca}(\text{OH})_2$ diffraction peaks were basically the same as that of the OPC paste, while the strengths of the C_3S and C_2S diffraction peaks had clearly decreased at 28 days. In addition, because of the vast amount of $\text{Ca}(\text{OH})_2$ that was formed, the hydration of the eco-cement pastes increased greatly, obviously enhancing the rate of the strength developing.

3.5. Porosity distribution in OPC and eco-cement pastes

The cumulative porosity for the three types of pastes, as obtained from the MIP tests, can be used to represent the total paste porosity. The porosities of the OPC and eco-cement A, B, and C pastes are shown in Figs. 5–8, respectively. The capillary pores ($>0.01 \mu\text{m}$) decreased continuously with curing time while the gel pores increased. At 28 days, the gel pores ($<0.01 \mu\text{m}$) in the eco-cement A paste increased with curing time. At 28 days, the gel porosity of the eco-cement C paste increased in volume similar to the plain paste (Fig. 8). This could be due to the presence of larger amounts of C_3S , the hydration product of the calcium silicate hydrates, which

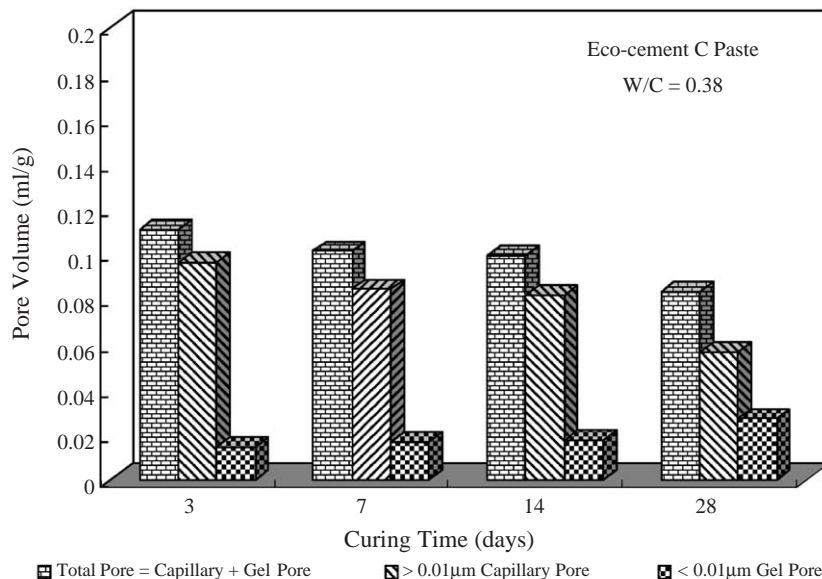


Fig. 8. Pore size distribution in eco-cement C pastes.

filled the capillary pores. At a curing age of 28 days, the volume percentage of fine pores in eco-cement B paste was less than in OPC paste (Fig. 7). One possible explanation for the pore size variation in eco-cement B paste was that the amount of α -C₂S led to the retardation of the early stages so the fine pore volume was less than in OPC paste.

4. Conclusions

From the studies carried out, the following conclusions can be drawn:

1. The leaching concentrations of all three types of eco-cement clinkers met the regulatory thresholds.
2. In the XRF analysis we note that SiO₂, CaO, Al₂O₃ were the primary components found in the eco-cement clinkers. Belite content in the clinker of eco-cement A clinker was similar that in OPC.
3. Eco-cement A paste had an initial setting time and final setting time similar to OPC paste.
4. Eco-cement B paste had an observed delay in the setting time which may be primary attributed to the larger amount of α -C₂S.
5. The compressive strength of OPC, eco-cement A and eco-cement B pastes occurred within the curing times. Eco-cement B clinker contained larger amounts of α -C₂S, which led to lower compressive strength.
6. From the porosity distribution, it was found that, at 28 days, the gel pores in the eco-cement A paste increased with curing time. Eco-cement B paste was that the amount of α -C₂S led to the retardation of the early stages so the fine pore volume was less than in OPC paste. At 28 days, the gel porosity of the eco-cement C paste increased in volume similar to the plain paste.

References

- [1] C.H. Weng, D.F. Lin, P.C. Chiang, Utilization of sludge as brick materials, *Adv. Environ. Res.* 7 (2003) 679–685.
- [2] J.H. Tay, Bricks manufactured from sludge, *J. Environ. Eng. ASCE* 113 (2) (1987) 278–283.
- [3] J.H. Tay, W.K. Yip, Sludge ash as lightweight concrete material, *J. Environ. Eng. ASCE* 115 (1) (1989) 56–64.
- [4] P.K. Mehta, Properties of blended cements, cements made from rice husk ash, *J. Am. Concr. Inst.* 74 (1997) 440–442.
- [5] P.K. Mehta, D. Pirtz, Use of rice husk to reduce temperature in high strength mass concrete, *J. Am. Concr. Inst.* 75 (1978) 60–63.
- [6] J.E. Aubert, B. Husson, A. Vaquier, Use of municipal solid waste incineration fly ash in concrete, *Cem. Concr. Res.* 34 (2004) 957–963.
- [7] J. Monzó, J.M. Payá, V.A. Borrachero, Use of sewage sludge ash (SSA)-cement admixtures in mortars, *Cem. Concr. Res.* 26 (9) (1996) 1389–1398.
- [8] J.H. Tay, Sludge ash as filler for Portland cement concrete, *J. Environ. Eng. Div. ASCE* 113 (1987) 345–351.
- [9] J.H. Tay, K.Y. Show, Clay blended sludge as lightweight aggregate concrete material, *J. Environ. Eng. ASCE* 117 (1991) 834–844.
- [10] J.E. Allemann, N.A. Berman, Constructive sludge management: biobrick, *J. Environ. Eng. ASCE* 110 (1984) 301–311.
- [11] J.I. Bhatti, J.K. Reid, Compressive strength of municipal sludge ash mortars, *ACI Mater.* 86 (1989) 394–400.
- [12] A. Idris, K. Saed, Characteristics of slag produced from incinerated hospital waste, *J. Hazard. Mater.* 93 (2002) 201–208.
- [13] J.H. Tay, K.Y. Show, Resource recovery of sludge as a building and construction material—a future trend in sludge management, *Water Sci. Technol.* 17 (1997) 259–266.
- [14] J. Majling, D.M. Roy, The potential of fly ash for cement manufacture, *Am. Ceram. Soc. Bull.* 72 (10) (1993) 77–81.
- [15] K. Miura, K. Sato, T. Suzuki, T. Oogami, A. Yazawa, Thermodynamic consideration on the kiln dust generated from eco-cement production, *Mat. Translmen* 42 (12) (2001) 2523–2530.
- [16] E. Proverbio, F. Carassiti, Evaluation of chloride content in concrete by X-ray fluorescence, *Cem. Concr. Res.* 27 (8) (1997) 1213–1223.
- [17] W.H. Duda, The Portland Cement Association: Research and Development, Construction Technology Laboratories, Skokie, IL, USA, 1975.
- [18] C. Jefferson, A.S. Jorge, Laboratory testing of the use of phosphate-coating sludge in cement clinker, *Resour. Conserv. Recycl.* 29 (2000) 169–179.